

EFFECT OF DIESEL-BIODIESEL-ETHANOL MIXTURES ON CORROSION RATE OF VARIOUS METALS IN THE PRESENCE OF *TERT*-BUTYLHYDROQUINONE (TBHQ)Chaza Joumaa^{a,*}, Ibtissam Saad^a and Ghassan Younes^a^aDepartment of Chemistry, Faculty of Science, Beirut Arab University, Debbiyeh, Lebanon

Recebido em 07/02/2023; aceito em 14/06/2023; publicado na web 27/07/2023

For many years, the goal of transitioning from conventional to renewable fuels (bioethanol and biodiesel) has been encouraged by government entities. However, due to the hygroscopicity of ethanol, ethanol/biodiesel blends can accelerate corrosion in metallurgy. Therefore, inhibitors can be added to mitigate corrosion. This research studied the effect of adding ethanol to diesel/biodiesel blends and measured the rate of corrosion on various metals (aluminum, copper, and 304 stainless steel) by the electrochemical impedance spectroscopy (EIS) method. The results indicated the corrosion rate increased with increasing the percentage of ethanol in the blends, and the corrosion inhibition efficiency of *tert*-butylhydroquinone (TBHQ) decreased upon the addition of ethanol. TBHQ was most effective as a corrosion inhibitor in the B15E5 blend. The inhibition efficiency of TBHQ decrease with the increase of the temperature. The adsorption process and the electrochemical parameters were calculated and discussed.

Keywords: DBE blend; corrosion; electrochemical impedance spectroscopy; *tert*-butylhydroquinone.

INTRODUCTION

The Renewable Fuel Standard (RFS) program in the United States requires refiners to blend biofuels into the fuel pool, aiming at replacing 36 billion gallons of fuel by renewable biofuels by 2022.¹ This program is one of many programs worldwide, which emphasize the role of biofuels in the transition phase to a clean renewable energy source. Biofuels, especially ethanol/bioethanol and biodiesel have gained progressive importance as alternative fuels for internal combustion engines.² They are biodegradable, non-toxic and cost efficient. The blends of diesel and ethanol could be used in existing diesel engines without engine modification in a very convenient way.³

However, the major drawback in diesel-ethanol (DE) fuel blends is the immiscibility of ethanol in diesel over a wide temperature range because of their chemical structure and characteristics. These can result in fuel instability due to phase separation. However, biodiesel is successfully added to DE blends to prevent phase separation and instability.⁴ Biodiesel is highly miscible in both diesel and ethanol; moreover, the addition of biodiesel to DE can act as an emulsifier forming new diesel-biodiesel-ethanol (DBE) blend, which can be used in diesel engines. This addition dramatically improves the solubility of ethanol in diesel over a wide range of temperature, and the DBE fuel blends are stable at temperatures well below zero.⁵

Different studies proved that the DBE blends have better properties and produce less harmful emissions than biodiesel diesel blends.^{6,7} Nevertheless, the auto-oxidation of biodiesel caused by its structure⁸ and the high hygroscopic nature of ethanol give the DBE blend its corrosive properties and makes the blends more susceptible to degradation, thus results in corrosion of the automobile fuel system parts.⁹

The diesel engine components that come into contact with the fuel are made from a variety of metals, non-metals and elastomers. The main parts of diesel engine components are made from steel (such as fuel tank, pump ring, fuel tube outlet and valve bodies), copper (such as fuel tank gasket, washer, and bushing), and aluminum (such as fuel pump, fuel filters and fuel pump) are normally affected by the

fuel blends.¹⁰ Thus, there is a great importance to study the corrosion susceptibility of these metals in DBE blends. To solve this major drawback and reduce the corrosiveness of biofuel, it is necessary to reduce its oxidation potential, which can be achieved by many approaches such as low temperature storage, enzyme deactivation, reducing partial pressure of oxygen in contact, inert gas packaging, vacuum technology or the use of antioxidants. Currently, most of the protection techniques can be expensive and require excessive energy. With that being said, antioxidants have been added to biofuels to retard or inhibit the corrosiveness of biodiesel.¹¹ Organic antioxidant containing oxygen, nitrogen and cyclic compounds are widely used.^{12,13} TBHQ (shown in Figure 1) is a phenolic antioxidant soluble in fat bearing hydroxyl groups and an aromatic ring in its structure both of which can facilitate its adsorption on the metal surface.¹⁴ TBHQ is used in the food industry as a preservative for unsaturated oils.^{11,15} It is also used as an additive in perfumes, resins, varnishes, as well as an effective antioxidant employed in many types of biofuels.¹⁶

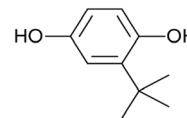


Figure 1. The molecular structure of TBHQ

Moreover, TBHQ has been found effective as a corrosion inhibitor toward carbon steel and galvanized steel in biodiesel.^{16,17} A preliminary investigation on the effect of TBHQ on the corrosion behavior of aluminum (Al), copper (Cu) and 304 stainless steel (SS) in biodiesel blend (B20) showed effective corrosion inhibition by TBHQ with the percentage inhibition of 61.52, 66.96 and 46.36% respectively at 4×10^{-6} mol dm⁻³ for Al, 1×10^{-4} mol dm⁻³ for Cu and 8×10^{-3} mol dm⁻³ for SS.¹⁸ However, the corrosion inhibition efficiency of TBHQ was not previously investigated in DBE blends. Therefore, the objective of the current study is to investigate the inhibition effect of TBHQ on the corrosion of four different proportions of DBE blends toward Al, Cu and SS using the electrochemical impedance spectroscopy technique (EIS).

*e-mail: chj349@student.bau.edu.lb

EXPERIMENTAL PART

Materials and methods

The biodiesel was prepared in the laboratory by transesterification of corn oil (acquired from a local store) with methanol (acquired from Sigma Aldrich), in the presence of NaOH as a catalyst. The reaction was done at 60 °C for 1 h, and biodiesel (product) and glycerol (byproduct) were separated in a separating funnel. The biodiesel was then washed with distilled water to remove all impurities. The properties of biodiesel are shown in Table 2 and these values were acceptable considering ASTM D6751-20a.

Diesel, biodiesel and ethanol 99.7% (acquired from Sigma-Aldrich) were mixed by volume in different proportions. The four different fuel blends, namely, B20 (80% diesel and 20% biodiesel), B15E5 (80% diesel, 15% biodiesel and 5% ethanol), B10E10 (80% diesel, 10% biodiesel and 10% ethanol) and B5E15 (80% diesel, 5% biodiesel and 15% ethanol) were prepared 30 minutes before the experiment (to prevent reaction of blend with oxygen atmosphere) and kept in sealed glass bottles. The properties of the pure biofuel and the various blends were determined according to American Society for Testing and Materials (ASTM) standards.

The working electrodes used were aluminum (Al), copper (Cu) and stainless steel (SS). The surface of the exposed area of each electrode was 9.15 cm². The chemical composition of all working electrodes was determined using Spectromax arc/spark OES metal analyzer present in TQP Laboratories, Lebanon, and is presented in Table 1. Each electrode was abraded before use with grading papers (grades 150, 350, 600 and 800) to remove the scratches produced during cutting and grinding, and thereafter washed with distilled water, rinsed with acetone and dried before the immersion in the blend.

In addition, TBHQ was acquired from Sigma Aldrich and used without any further purification.

Electrochemical testing was carried out in an electrochemical cell of two-electrode mode: one is connected to auxiliary and reference

terminals and the other to the working electrode terminal. The used potentiostat was Ivium Vertex One Technologies with serial No. of V01302 (the frequency range for EIS measurements was from 0.01 to 9.6×10^4 Hz with an applied potential signal amplitude of ± 10 mV around the rest potential). The AC experiment was conducted in the frequency range of 300,000 Hz-1 Hz at open circuit potential with amplitude of 10 mV peak-to-peak using AC signals. Before the electrochemical measurements, the specimens were immersed in test solution at open circuit potential for 20 min to attain a stable state.

RESULTS AND DISCUSSION

Fuel properties

The properties of biodiesel blends are very important for the efficient work of engines; the studies have shown that the addition of biodiesel can increase the density and viscosity of diesel, and change its cold weather properties, which can lead to undesirable consequences. However, the addition of ethanol can compensate for the slight change in the fuel properties. Density is one of the most important characteristics of fuel, where a high density can cause a change in engine output power due to the change in mass injected fuel since the fuel injection meter in the engine measure fuel by volume.^{9,19} As shown in Table 3, the density decreased upon addition of ethanol for a maximum of 1.83%. Another important parameter to assess in fuel quality is viscosity. High viscosity can cause poor fuel atomization, higher engine deposits and incomplete combustion.²⁰ In the current study, viscosity decreases by the addition of ethanol to a maximum of 28.62%. The cold flow properties such pour point can depict the cold flow operability of the fuel especially in cold weather.⁹ A decrease of 25% was observed in pour point. On the other hand, a slight increase (0.47%) was detected in the heat of combustion. Moreover, the sulfur content did not change suggesting that neither the biodiesel nor ethanol contain residual sulfur, leading to less harmful emission from the blends in comparison with conventional

Table 1. Chemical analysis of the used aluminum, copper and stainless steel specimens

Element	Mg	C	Si	Mn	P	Na	S	Ni	Cr	Al	Cu	Fe
Al wt. (%)	0.001	--	0.052	0.011	0.001	0.016	--	0.005	0.004	99.40	--	--
Cu wt. (%)	0.001	--	0.003	--	--	--	--	0.005	0.001	--	99.80	--
SS wt. (%)	--	0.045	0.485	1.640	0.001	--	0.003	7.590	19.83	--	--	68.30

Table 2. The properties of pure biodiesel

ASTM method	Property	Limits	Results
D4052	Density at 15 °C (kg m ⁻³)	report	887.7
D93	Flash point Pensky Martens (°C)	Min. 93	124
D2709	Water and sediment by centrifuge (% vol.)	Max. 0.05	Nil
D2500	Cloud point (°C)	report	-1
D445	Kinematic viscosity at 40 °C (cSt)	Min. 1.9 Max. 6.0	4.7
D5453	Sulfur (ppm)	Max. 15	1.7
D130	Corrosion copper strip (3 hours at 50 °C)	Max. 3	1A
D189	Carbon residue (% mass)	Max. 0.05	0.046
D974	Acid number (mg KOH g ⁻¹)	Max. 0.5	0.18
EN14538	Sodium and potassium combined (ppm)	Max. 5	0.024

Table 3. The properties of DBE blends

Properties	B20	B15E5	B10E10	B5E15	Method
Density at 15 °C (kg m ⁻³)	843.3	838.0	832.8	827.9	ASTM D4052
Kinematic viscosity at 40 °C (mm ² s ⁻¹)	2.90	2.53	2.28	2.07	ASTM D445
Flash point (°C)	71	16	14	13	ASTM D93
Pour point (°C)	-18	-21	-24	-24	ASTM D97
Sulfur (ppm)	4.5	4.5	4.5	4.5	ASTM D5453
Heat of combustion (MJ kg ⁻¹)	42.8	42.9	42.9	43.0	ASTM D2450

diesel. Nevertheless, there was a significant decrease of the flash point to below the ambient temperature, which is dominated by the flash point of the ethanol, this decrease makes the blends highly flammable which will lead to a change in the storage classification of the fuel and more precaution in the handling and transportations of the blends.¹⁹

EIS measurements

EIS is a non-destructive method used to study the electrochemical system and to predict the corrosion rate of metals. It was used to investigate the corrosion inhibition efficiency of TBHQ toward Al, Cu and 304 SS in four different DBE blend proportions. Figures 2, 3 and 4 show the Nyquist impedance plots for Al, Cu and 304 SS in B20, B15E5, B10E10 and B5E15, respectively, in the absence and presence of optimum concentrations of TBHQ at 30 °C.¹⁸

It can be observed that the impedance plots for all metals in the different DBE blends consisted of characteristic depressed semicircle of capacitive type indicating that the dissolution process occurs under activation control. The deviation from a typical semicircle is attributed to inhomogeneity and roughness of the metal surface.^{21,22} The presence of only one depressed semicircle suggests a single charge transfer process. Addition of TBHQ enlarged the diameter of the semicircle of the Nyquist plots without affecting the plot shape.¹⁸ This suggests that the inhibitive action of TBHQ is due to the adsorption of TBHQ molecules on the metal surfaces (Al, Cu and SS) without variation in the corrosion mechanism.²³ While the size of the obtained semicircle increased

upon addition of TBHQ, a significant decrease was observed with the increase of ethanol percentage in the blend for the three studied metals.

The impedance data of Al, Cu and SS in DBE blends are analyzed in terms of equivalent circuit model presented in Figure 5. It comprises a solution resistance (R_s), charge transfer resistance (R_{ct}) and constant phase element (CPE).²⁴ The CPE ($Q_{dl,n}$) is composed of non-ideal double layer capacitance Q_{dl} and a coefficient “n” that quantifies different physical phenomena like surface inhomogeneity, inhibitor adsorption and porous layer formation. The values of EIS parameters obtained from the fitting of the experimental Al, Cu and SS data to the corresponding equivalent circuit are indicated in Tables 4, 5 and 6, respectively.

The corrosion inhibition of TBHQ (% P) in DBE blends was estimated as follows:²⁵

$$\% P = [(R_{ct} - R_{ct0})/R_{ct}] \times 100 \quad (1)$$

where R_{ct} and R_{ct0} are the charge transfer resistance values (Gohm cm²) with and without TBHQ, respectively. The calculated values of % P in different DBE blends are indicated in Tables 4, 5 and 6, respectively.

It is evident that the R_{ct} values of the inhibited metals in all DBE blends were higher than the uninhibited metals, suggesting that the inhibition efficiency increases with the addition of TBHQ, while the corrosion rate decreases. The change in the R_{ct} and Q_{dl} values is due to the gradual replacement of the solution molecules by the organic

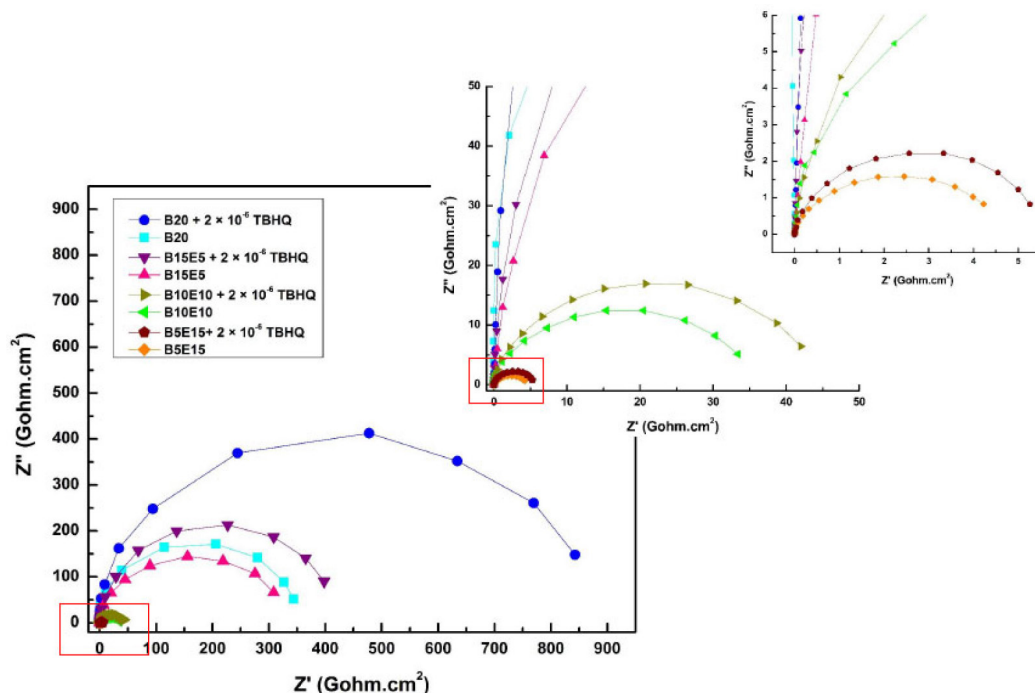


Figure 2. Nyquist impedance plots for aluminum in different proportions of DBE blends in the absence and the presence of TBHQ at 30 °C

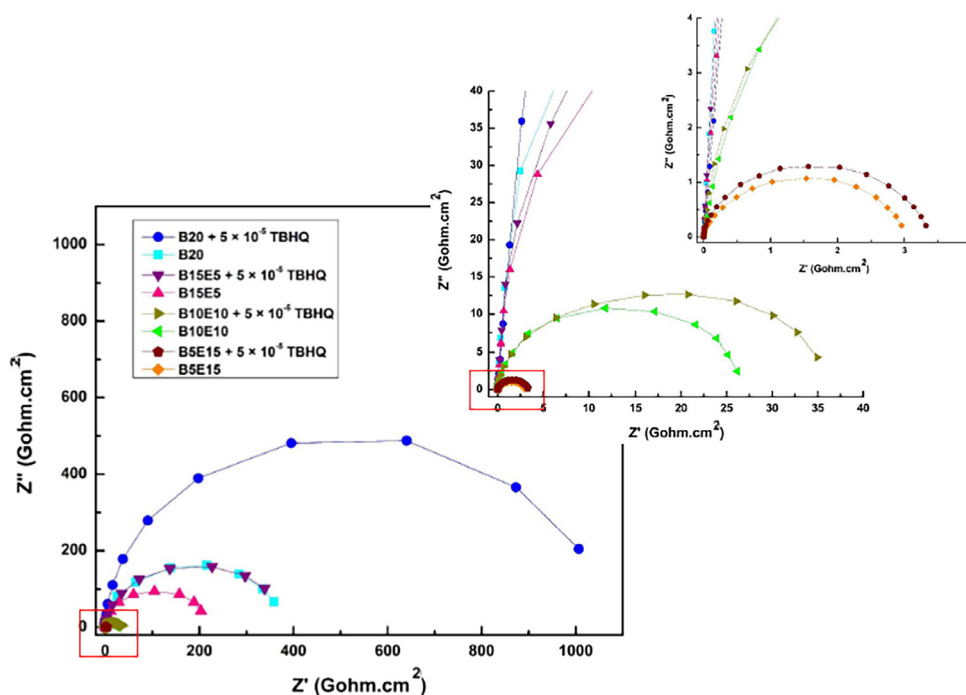


Figure 3. Nyquist impedance plots for copper in different proportions of DBE blends in the absence and the presence of TBHQ at 30 °C

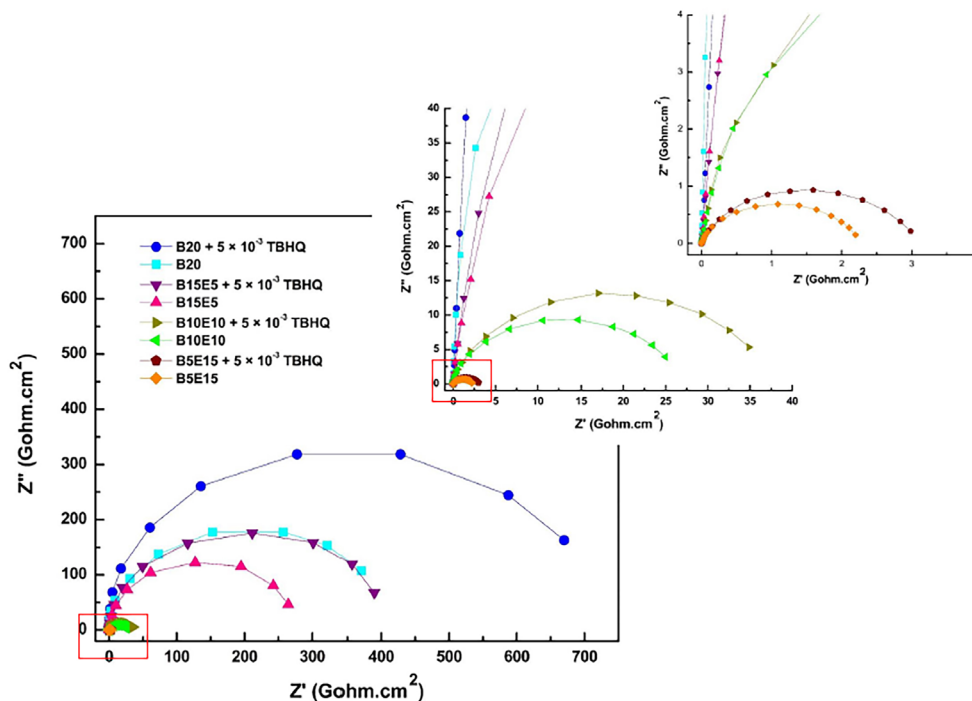


Figure 4. Nyquist impedance plots for 304 stainless steel in different proportions of DBE blends in the absence and the presence of TBHQ at 30 °C

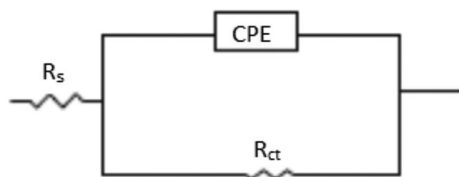


Figure 5. Schematic for the equivalent circuit model used to fit the impedance data

molecules on the metal surface, thus decreasing the extent of the metal dissolution. The decrease in Q_{dl} values with TBHQ addition is due to

the decrease in dielectric constant and/or increase in the thickness of the electrical double layer, which may imply that TBHQ molecules act by adsorption at the metal/solution interface.²⁵ Furthermore, it can be seen that corrosion increases with increasing the ethanol content in the DBE blends (going from B20 to B5E15) for the three studied metals, thus decreasing the corrosion inhibition efficiency of TBHQ significantly. This suggested that ethanol decreases the ability of TBHQ to adsorb on the surface of the metals. As corrosion mainly occurs due to presence of water in the blends, adding the hygroscopic ethanol leads to an increase in the moisture content that accelerates the corrosion rate. Moreover, the maximum inhibition in diesel-biodiesel-ethanol was observed by

Table 4. Electrochemical impedance parameters for the corrosion of Al in DBE blend in the absence and the presence of TBHQ at 30 °C

Blend	Solution (mol L ⁻¹)	R _s (Gohm cm ²)	R _{ct} (Gohm cm ²)	n	Q _{dl} (μF cm ²)	P (%)
B20	Blank	0.02	387	1.00	6.33 × 10 ⁻¹¹	---
	TBHQ	0.01	952	0.97	2.78 × 10 ⁻¹¹	59.39
B15E5	Blank	0.01	367	0.90	7.65 × 10 ⁻¹¹	---
	TBHQ	0.01	488	0.91	5.22 × 10 ⁻¹¹	24.86
B10E10	Blank	0.01	40.2	0.75	4.25 × 10 ⁻¹⁰	---
	TBHQ	0.01	51.7	0.74	3.06 × 10 ⁻¹⁰	22.26
B5E15	Blank	0.02	5.32	0.70	2.51 × 10 ⁻⁹	---
	TBHQ	0.02	6.52	0.73	1.80 × 10 ⁻⁹	18.44

Table 5. Electrochemical impedance parameters for the corrosion of Cu in DBE blend in the absence and the presence of TBHQ at 30 °C

Blend	Solution (mol L ⁻¹)	R _s (Gohm cm ²)	R _{ct} (Gohm cm ²)	n	Q _{dl} (μF cm ²)	P (%)
B20	Blank	0.01	413	0.92	5.44 × 10 ⁻¹¹	---
	TBHQ	0.02	1140	0.97	3.05 × 10 ⁻¹¹	63.79
B15E5	Blank	0.01	241	0.91	1.10 × 10 ⁻¹⁰	---
	TBHQ	0.01	421	0.90	8.40 × 10 ⁻¹¹	42.66
B10E10	Blank	0.01	29.7	0.86	3.66 × 10 ⁻¹⁰	---
	TBHQ	0.01	41.1	0.76	2.92 × 10 ⁻¹⁰	27.75
B5E15	Blank	0.02	3.41	0.73	1.87 × 10 ⁻⁹	---
	TBHQ	0.02	3.84	0.71	1.21 × 10 ⁻⁹	11.16

Table 6. Electrochemical impedance parameters for the corrosion of SS in DBE blend in the absence and the presence of TBHQ at 30 °C

Blend	Solution (mol L ⁻¹)	R _s (Gohm cm ²)	R _{ct} (Gohm cm ²)	n	Q _{dl} (μF cm ²)	P (%)
B20	Blank	0.01	457	0.92	7.92 × 10 ⁻¹¹	---
	TBHQ	0.02	784	0.95	4.42 × 10 ⁻¹¹	41.74
B15E5	Blank	0.01	297	0.97	9.87 × 10 ⁻¹¹	---
	TBHQ	0.01	442	0.94	5.86 × 10 ⁻¹¹	32.82
B10E10	Blank	0.01	29.4	0.77	4.38 × 10 ⁻¹⁰	---
	TBHQ	0.01	41.8	0.73	2.87 × 10 ⁻¹⁰	29.70
B5E15	Blank	0.02	2.46	0.72	2.70 × 10 ⁻⁹	---
	TBHQ	0.02	3.36	0.70	2.43 × 10 ⁻⁹	26.87

using B15E5 blend for three used metals, and the TBHQ had the most efficiency with the lowest ethanol percentage.

Effect of temperature

Based on the above data and findings, the B15E5 was the least corrosive blend. The effect of temperature using TBHQ as corrosion inhibitor in B15E5 blend was investigated by EIS measurements in the temperature range 303-333 K. Figures 6(a) and 6(b) show the Nyquist plots obtained for Cu in B15E5, in the absence and the presence of TBHQ at different temperatures. An increase in temperature resulted in a depression in the size of the semicircles, indicating a decrease in the charge transfer resistance (R_{ct}) values. Similar behavior was observed for Al and SS in B15E5 blend.

This indicates that the corrosion rate increases with the increase in temperature both in uninhibited and inhibited solutions. The decrease in the inhibition efficiency can be attributed to increases rate of dissolution process of metal and partial desorption of the inhibitor from the metal surface with an increase in temperature.²⁶

Activation and thermodynamic parameters

The activation and thermodynamic parameters are of great importance for elucidating the mechanism of corrosion inhibition of the three metals. The activation and thermodynamic parameters for Al, Cu and SS corrosion in B15E5 in the absence and presence of different concentrations TBHQ were obtained by applying Arrhenius type plot (Equation 2) and transition state (Equation 3):²⁵

$$\ln v = \ln A - (E_a/RT) \quad (2)$$

where v is the corrosion rate, E_a is apparent activation energy, A is the pre-exponential factor, and R is the universal gas constant.

$$v = RT/Nh e^{\Delta S^*/R} \times e^{-\Delta H^*/RT} \quad (3)$$

where ΔH^* is the apparent enthalpy of activation, ΔS^* is the apparent entropy of activation, h is the Planck's constant and N is the

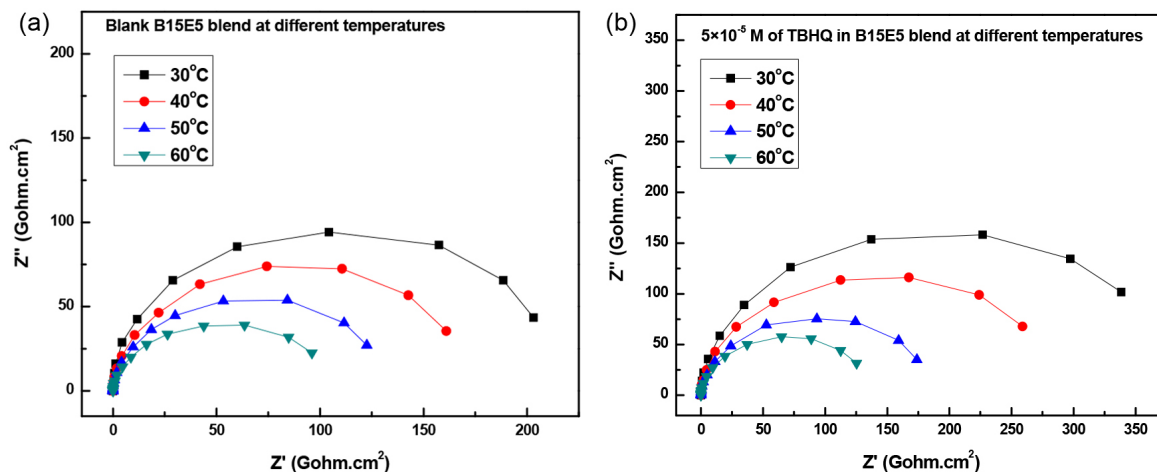


Figure 6. Nyquist impedance plots for Cu in B15E5 blend in (a) the absence and (b) the presence of $5 \times 10^{-5} \text{ mol dm}^{-3}$ of TBHQ at different temperatures

Avogadro's number, and T the thermodynamic temperature.

A plot of $\ln(v)$ versus $(1/T)$ gave a straight line as shown in Figure 7 with a slope of $-E_a/R$ for the three tested metals. The values of activation energy are presented in Table 7. The data showed that the activation energy of Al, Cu and SS in B15E5 in the presence of TBHQ is higher than that of the blank solutions (B15E5). This increase suggested a protective effect of TBHQ molecules on the three metal surfaces. The activation energy with Cu is higher than that with Al and SS reflecting high protection efficiency for Cu compared to the other two metals.

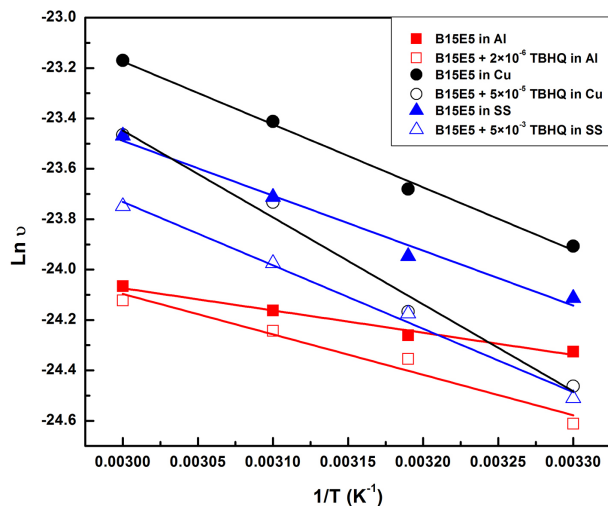


Figure 7. Variation of $\ln v$ with $1/T$ of Al, Cu and 304 SS in B15E5 in the absence and the presence of TBHQ

Moreover, a plot of $\ln(v/T)$ versus $(1/T)$ gave a straight line as shown in Figure 8 with a slope of $(-\Delta H^*/R)$ and intercept of $(\ln R/Nh + \Delta S^*/R)$. From the slope and intercept, ΔH^* and ΔS^* were calculated and their values are given in Table 7. The positive sign of enthalpies ΔH^* reflect the endothermic nature of the metals dissolution process.²⁷ Moreover, the presence of the inhibitor produces higher value of ΔH^* than those obtained for the uninhibited solutions. This suggests that metal dissolution in B15E5 requires more energy in the presence of the inhibitor TBHQ. Higher values of ΔH^* using copper metal means that the dissolution of copper in B15E5 blend in the presence of TBHQ is difficult compared to the other two metals, thus corroborating the conclusions drawn from the activation energy data. In addition, the negative and large values of ΔS^* implies that the activation complex represents an association rather than a dissolution

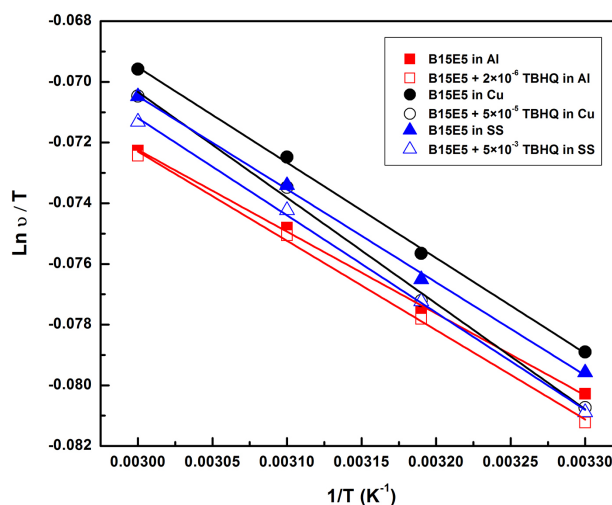


Figure 8. Variation of $\ln(v/T)$ with $1/T$ of Al, Cu and 304 SS in B15E5 in the absence and the presence of TBHQ

Table 7. Activation parameters of the dissolution of Al, Cu and SS in B15E5 in the absence and presence of TBHQ

Metal	Inhibitor	E_a (kJ mol ⁻¹)	ΔH^* (J mol ⁻¹)	ΔS^* (J mol ⁻¹ K ⁻¹)
Al	Blank	7340.7	224.23	-197.468
	TBHQ	13338.4	244.67	-197.407
Cu	Blank	20765.5	261.16	-197.335
	TBHQ	28689.9	289.72	-197.256
SS	Blank	18124.4	254.94	-197.361
	TBHQ	20935.4	266.45	-197.333

step, and inferred that a decrease in disorder takes place on going from reactants to activated complex.²⁸

CONCLUSION

Different metals (Al, Cu, and SS) have shown variation in corrosion rates with increasing ethanol concentration in the blends. The addition of ethanol was found to increase the rate of corrosion for all metals. TBHQ was an effective corrosion inhibitor and showed good performance on Al, Cu and SS in the four different proportions of DBE blends as suggested by the electrochemical impedance measurements. Nevertheless, the inhibition efficiency of TBHQ decreased with

increasing ethanol content. In addition, at 60 °C, the corrosion of metals in DBE blends is higher than at room temperature. Higher activation energy of Al, Cu and SS in different DBE blends was obtained in the presence of the inhibitor TBHQ with positive sign of enthalpies ΔH^* that reflected the endothermic nature of the metals dissolution process.

REFERENCES

1. <https://crsreports.congress.gov/product/pdf/R/R43325>, accessed in July 2023.
2. Demirbas, A.; *Appl. Energy* **2011**, *88*, 17. [Crossref]
3. Faried, M.; Samer, M.; Abdelsalam, E.; Yousef, R. S.; Attia, Y. A.; Ali, A. S.; *Renewable Sustainable Energy Rev.* **2017**, *79*, 893. [Crossref]
4. Lapuerta, M.; Armas, O.; García-Contreras, R.; *Fuel* **2007**, *86*, 1357. [Crossref]
5. Shahir, S. A.; Masjuki, H. H.; Kalam, M. A.; Imran, A.; Fattah, I. M. R.; Sanjid, A.; *Renewable Sustainable Energy Rev.* **2014**, *32*, 379. [Crossref]
6. Kwanchareon, P.; Luengnaruemitchai, A.; Jai-In, S.; *Fuel* **2007**, *86*, 1053. [Crossref]
7. Hussan, M. J.; Hassan, M. H.; Kalam, M. A.; Memon, L. A.; *J. Cleaner Prod.* **2013**, *51*, 118. [Crossref]
8. Singh, B.; Korstad, J.; Sharma, Y. C.; *Renewable Sustainable Energy Rev.* **2012**, *16*, 3401. [Crossref]
9. Ali, O.; Mamat, R.; Abdullah, N. R.; Adam, A.; Khoerunnisa, F.; Sardjono, R. E.; *MATEC Web of Conferences* **2016**, *38*, 03002. [Crossref]
10. Haseeb, A. S. M. A.; Fazal, M. A.; Jahirul, M. I.; Masjuki, H. H.; *Fuel* **2011**, *90*, 922. [Crossref]
11. Varatharajan, K.; Pushparani, D. S.; *Renewable Sustainable Energy Rev.* **2018**, *82*, 2017. [Crossref]
12. Bahrami, M. J.; Hosseini, S. M. A.; Pilvar, P.; *Corros. Sci.* **2010**, *52*, 2793. [Crossref]
13. Hijazi, K. M.; Abdel-Gaber, A. M.; Younes, G. O.; Habchi, R.; *Port. Electrochim. Acta* **2021**, *39*, 4. [Crossref]
14. Cook, E. L.; Hackerman, N.; *J. Phys. Chem.* **1951**, *55*, 549. [Crossref]
15. Prasad, N.; Siddaramaiah, B.; Banu, M.; *J. Food Sci. Technol.* **2015**, *52*, 2238. [Crossref]
16. Fernandes, D. M.; Montes, R. H. O.; Almeida, E. S.; Nascimento, A. N.; Oliveira, P. V.; Richter, E. M.; Muñoz, R. A. A.; *Fuel* **2013**, *107*, 609. [Crossref]
17. Fernandes, D. M.; Squizzato, A. L.; Lima, A. F.; Richter, E. M.; Munoz, R. A. A.; *Renewable Energy* **2019**, *139*, 1263. [Crossref]
18. Joumaa, C.; Saad, I.; Younes, G.; *BAU Journal - Science and Technology* **2021**, *3*, 1. [Crossref]
19. Barabas, I.; Todoruț, A.; *SAE 2009 Powertrains, Fuels and Lubricants Meeting*, Texas, USA, 2009. [Crossref]
20. Barabas, I.; Todoruț, I. A. In *Biodiesel - Quality, Emissions and By-Products*; Montero, G.; Stoytcheva, M., eds.; IntechOpen: London, 2011, ch.14.
21. Deyab, M. A.; Corrêa, R. G. C.; Mazzetto, S. E.; Dhmees, A. S.; Mele, G.; *Ind. Crops Prod.* **2019**, *130*, 146. [Crossref]
22. Sayed, M. Y. E.; Ghouch, N. E.; Younes, G. O.; Awad, R.; *Journal of Bio- and Tribo-Corrosion* **2022**, *8*, 4. [Crossref]
23. Tan, K. W.; Kassim, M. J.; Oo, C. W.; *Corros. Sci.* **2012**, *65*, 152. [Crossref]
24. Kilo, M.; Rahal, H. T.; El-Dakdouki, M. H.; Abdel-Gaber, A. M.; *Chem. Eng. Commun.* **2021**, *208*, 1676. [Crossref]
25. Umoren, S. A.; Banera, M. J.; Alonso-Garcia, T.; Gervasi, C. A.; Mirficio, M. V.; *Cellulose* **2013**, *20*, 2529. [Crossref]
26. Schorr, M.; Yahalom, J.; *Corros. Sci.* **1972**, *12*, 867. [Crossref]
27. Mu, G.; Li, X.; Li, F.; *Mater. Chem. Phys.* **2004**, *86*, 59. [Crossref]
28. Deyab, M. A.; *J. Ind. Eng. Chem.* **2015**, *22*, 384. [Crossref]

